

Analytical dispersive parameterization for elastic scattering of spinless particles

Igor Danilkin^a, Volodymyr Biloshytskyi^a, Xiu-Lei Ren^{a,b}, Marc Vanderhaeghen^a

^a*Institut für Kernphysik & PRISMA⁺ Cluster of Excellence, Johannes Gutenberg Universität, D-55099 Mainz, Germany*

^b*Helmholtz Institut Mainz, D-55099 Mainz, Germany*

Abstract

In this letter, we present a novel parameterization of the elastic scattering of spin-0 particles, which is based on a dispersive representation for the inverse amplitude. While the right-hand cut is controlled by unitarity, the contribution from the left-hand cut can be parameterized using the expansion in a suitably constructed conformal variable, which accounts for its analytic structure. The inclusion of the Adler zero and threshold factors for $J > 0$ are discussed in detail and as well as its numerical implementation. The proposed dispersive amplitudes are written in a compact analytic form and provide a powerful tool to analyse current and future lattice data in the elastic region improving on the commonly used Breit-Wigner or K-matrix approaches.

1. Introduction

Over the last decade there is a renewed interest in the hadron spectroscopy, motivated by recent discoveries of unexpected exotic hadron resonances [1–3]. At the same time, there is significant progress in lattice QCD studies of excited hadrons [4], which has a great potential for determining the properties of the poorly known hadronic states.

The determination of resonance parameters requires the search for poles in the complex plane. This is particularly important when there is an interplay between several inelastic channels or when the pole is very deep in the complex plane. The fundamental S-matrix constraints, such as unitarity, analyticity, and crossing symmetry significantly constrain the possible form of the amplitude both on the real axis and in the complex plane [5]. Unfortunately, in the experimental and lattice analyses, it is a common practice to ignore most of the S-matrix constraints and rely on the different variants of Breit-Wigner or K-matrix parameterizations due to their simplicity [6–12]. Both methods ignore the existence of the left-hand cut and often lead to spurious poles in the complex plane. In addition, for a reaction involving Goldstone bosons, the Adler zero constraint is typically ignored or implemented purely phenomenologically (see e.g. parameterizations suggested in [13–15]). As a result, the systematic uncertainties of these approaches are large [16].

The most rigorous way of implementing all S-matrix constraints is to write a fixed- t dispersion relation for the invariant amplitude $T(s, t, u)$, which after projection onto partial waves leads to the set of Roy or Roy-Steiner equations [17]. In this way, the left-hand cut is treated exactly. In practical applications, however, the rigorous implementation of these equations is almost impossible, since it requires experimental knowledge of all partial waves with different isospin in the direct and crossed channels (including the high-energy region). Therefore, the current precision studies of $\pi\pi$ [18–21] and πK [22, 23] scattering are based on a finite truncation, which, in turn, limits the results to the given kinematic region. Furthermore, ap-

plying Roy-like equations for coupled-channel cases is relatively complicated and has not been achieved in the literature so far. In [24] we used a complementary approach, which is based on solving the partial wave (p.w.) dispersion relations. In this method, different partial waves with different isospins are fully decoupled, at the expense of the crossing symmetry constraint is not being incorporated exactly. The benefit of this approach is that it can be applied to any hadronic reaction, for which the data exist (experimental or lattice), and can be straightforwardly extended to the coupled-channel systems. For instance, one of the central results of [24] is the isoscalar coupled-channel $\{\pi\pi, K\bar{K}\}$ Omnès matrix. It does not have left-hand cuts and therefore serves as the crucial input for the vast production/decay reactions involving the same final states (see e.g. [25] and [26]).

Since some of the resonances are connected almost exclusively to the elastic channels (especially in the lattice calculations with unphysically-large masses for light quarks) it is not always necessary to solve the dispersive integral equation for the direct amplitude [24]. In this letter we propose a set of the novel parametrizations for elastic scattering, which, on one hand, respect dispersive relations, while on the other hand can be written in a compact analytic form with a few unknown parameters. The idea is to write a dispersion relation for the inverse amplitude and parameterize the left-hand cut contribution in the physical region by the conformal mapping expansion, which respects its analytical structure. The possible Adler zero of the amplitude is included as a pole of the inverse amplitude. In the derivation of the dispersive parametrization for the higher partial waves, we implement the angular momentum barrier factor as a relevant kinematic constraint. Moreover, we discuss in detail the equivalence of the p.w. dispersion relations for the direct and inverse amplitudes for elastic scattering. In this respect, we show that the commonly used modified Inverse Amplitude Method (mIAM) [27–30] satisfies the p.w. dispersion relation only for the inverse, but not for the direct amplitude due to two spurious poles on the first Riemann sheet. This

arXiv:2206.15223v1 [hep-ph] 30 Jun 2022

is not the case for the P-wave, where the IAM satisfies both dispersion representations.

Finally, we show some numerical test cases, with the emphasis on the recent lattice data on the S-wave isoscalar $\pi\pi \rightarrow \pi\pi$ scattering ($m_\pi = 236$ MeV) from the HadSpec collaboration [6].

2. Formalism

2.1. Unitarity

The s -channel partial-wave decomposition for $2 \rightarrow 2$ process is given by

$$T(s, t) = 16\pi N \sum_{J=0}^{\infty} (2J+1) t_J(s) P_J(\cos \theta), \quad (1)$$

where θ is the center-of-mass (c.m.) scattering angle. For the scattering of identical particles $N = 2$, while $N = 1$ otherwise. This factor is useful to ensure the same unitarity condition for the identical and non-identical two-particle scattering, which in the elastic approximation is given by

$$\begin{aligned} \text{Im } t_J(s) &= \rho(s) |t_J(s)|^2 \theta(s - s_{th}), \\ \text{Im } (t_J(s))^{-1} &= -\rho(s) \theta(s - s_{th}), \end{aligned} \quad (2)$$

where $s_{th} = (m_1 + m_2)^2$ is a threshold. The phase space factor $\rho(s)$ is given by

$$\rho(s) = \frac{2p(s)}{\sqrt{s}}, \quad (3)$$

where $p(s)$ is the c.m. three-momentum of the system

$$p(s) = \frac{\lambda^{1/2}(s, m_1^2, m_2^2)}{2\sqrt{s}} \equiv \sqrt{\frac{(s - m_+^2)(s - m_-^2)}{4s}}, \quad (4)$$

with λ being the Källén function and $m_\pm = m_1 \pm m_2$. At low energy, the effective range expansion for partial waves is conventionally defined as

$$\frac{2}{\sqrt{s_{th}}} \text{Re } t_J(s) \simeq p^{2J}(s) (a_J + b_J p^2(s) + \dots), \quad (5)$$

where a_J and b_J denote the scattering length and the slope parameter, respectively. At high energy, the unitarity condition (2) guarantees that the partial-wave amplitudes at infinity approach at most constants

$$-\frac{1}{2\rho(s)} \leq \text{Re } t_J(s) \leq \frac{1}{2\rho(s)}, \quad 0 \leq \text{Im } t_J(s) \leq \frac{1}{\rho(s)} \quad (6)$$

and in accordance with that, we assume throughout this work that

$$t_J(s \rightarrow \infty) \rightarrow \text{const}. \quad (7)$$

2.2. S-wave scattering

We start with an investigation of the S-wave ($J = 0$) scattering of spinless particles, since in this case we do not need to worry about angular momentum barrier factors. In view of the maximal analyticity assumption [31], the partial-wave amplitude satisfies, according to Eq. (7), the once-subtracted dispersion relation,

$$t_0(s) = t_0(s_M) + \frac{s - s_M}{\pi} \int_{L,R} \frac{ds'}{s' - s_M} \frac{\text{Im } t_0(s')}{s' - s} + \frac{s - s_M}{s_B - s_M} \frac{g_B^2}{s_B - s}. \quad (8)$$

The symbols L and R denote integrals over left- and right-hand cuts, respectively. The choice of the subtraction point at $s = s_M$ in general is irrelevant and will be discussed later. For completeness, we admit a possible bound state at $s = s_B$ with the coupling g_B . Using the unitarity relation (2) on the right-hand cut, Eq. (8) simplifies to

$$\begin{aligned} t_0(s) &= t_0(s_M) + \frac{s - s_M}{\pi} \int_L \frac{ds'}{s' - s_M} \frac{\text{Im } t_0(s')}{s' - s} \\ &+ \frac{s - s_M}{\pi} \int_{s_{th}}^{\infty} \frac{ds'}{s' - s_M} \frac{\rho(s') |t_0(s')|^2}{s' - s} + \frac{s - s_M}{s_B - s_M} \frac{g_B^2}{s_B - s}. \end{aligned} \quad (9)$$

The solution to (9) can be written using the N/D ansatz [32] where the contributions of left- and right-hand cuts are separated into $N(s)$ and $D(s)$ functions, respectively. This ansatz implies a set of linear integral equations [33, 34] which can be solved with the input from the left-hand cut [24].

Alternatively, for the elastic scattering one can write a partial wave dispersion relation for the inverse amplitude

$$\begin{aligned} [t_0(s)]^{-1} &= [t_0(\tilde{s}_M)]^{-1} + \frac{s - \tilde{s}_M}{\pi} \int_{L,R} \frac{ds'}{s' - \tilde{s}_M} \frac{\text{Im } [t_0(s')]^{-1}}{s' - s} \\ &+ \frac{s - \tilde{s}_M}{s_A - \tilde{s}_M} \frac{g_A}{s - s_A}, \end{aligned} \quad (10)$$

where we allowed for the pole contribution at $s = s_A$, which corresponds to the possible zero of the amplitude (e.g. Adler zero in $\pi\pi$ and πK scattering). The integral over the right-hand cut can be fixed again from unitarity in Eq. (2), leading to the following integral equation

$$\begin{aligned} [t_0(s)]^{-1} &= [t_0(\tilde{s}_M)]^{-1} + \frac{s - \tilde{s}_M}{\pi} \int_L \frac{ds'}{s' - \tilde{s}_M} \frac{\text{Im } [t_0(s')]^{-1}}{s' - s} \\ &+ \frac{s - \tilde{s}_M}{\pi} \int_{s_{th}}^{\infty} \frac{ds'}{s' - \tilde{s}_M} \frac{-\rho(s')}{s' - s} + \frac{s - \tilde{s}_M}{s_A - \tilde{s}_M} \frac{g_A}{s - s_A}. \end{aligned} \quad (11)$$

We emphasize that Eqs. (11) and (9) are equivalent: $t_0(s)$ and $[t_0(s)]^{-1}$ have the same analytic structure, except for the possible presence of poles (or zeros) in $t_0(s)$ and $[t_0(s)]^{-1}$. It could be a pole in $t_0(s)$ that correspond to the bound state and therefore $[t_0(s_B)]^{-1} = 0$. Another possibility is a pole in $[t_0(s)]^{-1}$, that correspond to the Adler zero, $t_0(s_A) = 0$. The constraints of $t_0(s_A) = 0$ and $[t_0(s_B)]^{-1} = 0$ can be easily incorporated in Eqs. (9) and (11) by choosing $s_M = s_A$ and $\tilde{s}_M = s_B$, respectively. We checked numerically for the elastic isoscalar $\pi\pi$ S-wave scattering that Eqs. (9) and (11) are consistent with each

other using a toy model for the left-hand cut discontinuity in Eq. (9).

In a general scattering problem, little is known about the left-hand cuts, except their analytic structure in the complex plane. The progress has been made in [35]. It relies on the consideration of an analytic continuation of the left-hand cut contributions to the physical region, employing a series expansion in terms of a suitably constructed conformal mapping variable $\omega(s)$. The latter is chosen such that it maps the left-hand cut plane onto the unit circle [36]. For the most typical cases the exact forms of $\omega(s)$ will be given in Sec.2.5. In [24] the first two terms of Eq. (9) were expanded in the conformal mapping series. Here we suggest to apply the conformal mapping expansion to the first two terms of Eq. (11), which leads to the following parametrization of the inverse of $t_0(s)$,

$$[t_0(s)]^{-1} \simeq \sum_{n=0}^{\infty} C_n \omega^n(s) + R(s, \tilde{s}_M) + \frac{s - \tilde{s}_M}{s_A - \tilde{s}_M} \frac{g_A}{s - s_A}, \quad (12)$$

where the analytical expression of

$$R(s, \tilde{s}_M) \equiv \frac{s - \tilde{s}_M}{\pi} \int_{s_{th}}^{\infty} \frac{ds'}{s' - \tilde{s}_M} \frac{-\rho(s')}{s' - s}, \quad (13)$$

is given in Appendix A. The unknown coefficients C_n , g_A and s_A can be adjusted to reproduce the experimental or lattice data or be fixed from the effective field theory by imposing some matching condition.

In general, the choice of the subtraction point $\tilde{s}_M \neq s_A$ is irrelevant. However, for the cases when the p.w. amplitude has an Adler zero, it is useful to subtract the dispersion relation at s_{th} . This choice and the truncated conformal expansion at $n_{max} = 0$, allows to connect C_0 parameter directly to the scattering length a_0 , given in Eq. (5),

$$n_{max} = 0, \quad C_0 = [t_0(s_{th})]^{-1} = \frac{2}{a_0 \sqrt{s_{th}}}. \quad (14)$$

As will be shown in Sec. 3, it is often enough to describe the data with just a constant term in the conformal expansion and Adler zero parameters.

The advantage of (11) compared to (9) in the elastic approximation is twofold. First of all, when in both dispersion representations the left-hand cut is approximated by the conformal expansion, Eq. (11) becomes much simpler than Eq. (9), because one does not need to solve numerically the integral equation. Secondly, as it will be shown below, it is easy to extend the formalism to $J \neq 0$. However, the dispersion relation for the inverse amplitude has a clear limitation: it cannot be extended to the coupled-channel case [37, 38]. Due to the matrix inversion, there would be a mixture of the left-hand cuts of all involved channels, which can also affect the physical region where one has an overlapping cut structure. The typical example is the coupled-channel $\{\pi\pi, K\bar{K}\}$ scattering [39], in which the left-hand cut of $K\bar{K} \rightarrow K\bar{K}$ starts at $4(m_K^2 - m_\pi^2)$ and the matrix inversion will therefore produce a spurious contribution to the $\pi\pi \rightarrow \pi\pi$ unitarity cut. In contrast, the overlapping of left and right hand cuts in $K\bar{K} \rightarrow K\bar{K}$ does not jeopardize the N/D framework, since it happens in the non-physical region (see Ref. [24] for more details and its application to $f_0(980)$).

2.3. $J \neq 0$, $m_1 = m_2$ scattering

For the case of scattering with $J \neq 0$ one needs to take into account the angular momentum barrier factor which implies that around the threshold the amplitude should behave as

$$t_J(s) \sim p(s)^{2J} \underset{\sim}{\sim} (s - s_{th})^J. \quad (15)$$

This is implemented by writing a $J + 1$ subtracted dispersion relation for the ratio

$$f_J(s) \equiv \frac{(s - s_{th})^J}{t_J(s)}, \quad (16)$$

which is free from kinematic constraints. It leads to

$$f_J(s) = \sum_{i=0}^J \frac{1}{i!} f_J^{(i)}(s_{th}) (s - s_{th})^i + \frac{(s - s_{th})^{J+1}}{\pi} \int_{L,R} \frac{ds'}{(s' - s_{th})^{J+1}} \frac{\text{Im } f_J(s')}{s' - s}, \quad (17)$$

where no Adler-related pole was added since there is no known reaction where the amplitude has an extra zero in addition to the $s = s_{th}$ given in Eq. (15). Note, that here we subtracted the dispersion relation at the threshold. It allows us to bring the integral over the right hand cut into the form of Eq. (13). Indeed, re-expressing $f_J(s)$ in terms of $t_J(s)$ and applying the unitarity relation (2), we obtain

$$[t_J(s)]^{-1} = \frac{1}{(s - s_{th})^J} \sum_{i=0}^J \frac{1}{i!} f_J^{(i)}(s_{th}) (s - s_{th})^i + \frac{s - s_{th}}{\pi} \int_L \frac{ds'}{s' - s_{th}} \frac{\text{Im } [t_J(s')]^{-1}}{s' - s} + \frac{s - s_{th}}{\pi} \int_{s_{th}}^{\infty} \frac{ds'}{s' - s_{th}} \frac{-\rho(s')}{s' - s}. \quad (18)$$

Since $f_J^{(i)}(s_{th})$ are in general unknown constants, one can write a general parametrization

$$[t_J(s)]^{-1} \simeq \frac{1}{(s - s_{th})^J} \sum_{i=0}^{J-1} \frac{1}{i!} f_J^{(i)}(s_{th}) (s - s_{th})^i + \sum_{n=0}^{\infty} C_n \omega^n(s) + R(s, s_{th}), \quad (19)$$

where as before, the contribution from the left-hand cut together with the constant term was expanded in a suitably constructed conformal mapping series. For instance, for $J = 1$ it corresponds to

$$[t_1(s)]^{-1} \simeq \frac{a}{s - s_{th}} + \sum_{n=0}^{\infty} C_n \omega^n(s) + R(s, s_{th}), \quad (20)$$

and similar for $J = 2$

$$[t_2(s)]^{-1} \simeq \frac{a}{(s - s_{th})^2} + \frac{b}{s - s_{th}} + \sum_{n=0}^{\infty} C_n \omega^n(s) + R(s, s_{th}). \quad (21)$$

The parameters a , b and C_n will be fitted to the data in Sec. 3.

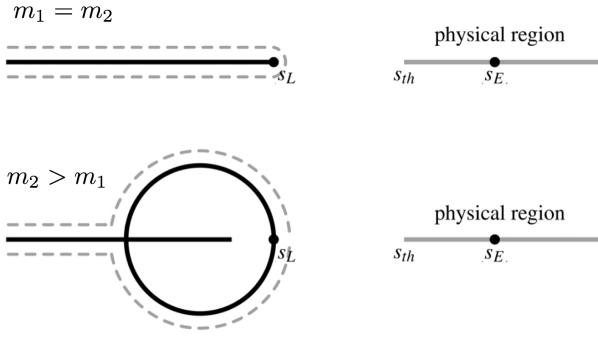


Figure 1: Left-hand cut singularities (solid black curves) in the complex s -plane for the case when $m_1 = m_2$ (upper plane) and $m_2 > m_1$ (lower plane). In the plot, we schematically show the position of the closest left-hand cut singularity (s_L), threshold (s_{th}), and the expansion point (s_E). Dashed lines determine the specific form of the conformal map and subsequently the domain of convergence of the conformal expansion.

2.4. $J = 1$, $m_1 \neq m_2$ scattering

In case of non-equal masses we propose to write a dispersion representation for the amplitude

$$g_J(s) \equiv \frac{p(s)^{2J}}{t_J(s)}, \quad (22)$$

which is free from any kinematic constraints. For simplicity, we limit ourselves only to the $J = 1$ case, with an example in mind of πK or πD scattering. For $J = 1$ we write a twice-subtracted dispersion relation for $g_1(s)$ in the following form

$$g_1(s) = a + b s + \frac{(s - m_+^2)(s - m_-^2)}{\pi} \int_{L,R} \frac{ds'}{(s' - m_+^2)(s' - m_-^2)} \frac{\text{Im } g_1(s')}{s' - s},$$

where $m_{\pm} = m_1 \pm m_2$. Re-expressing $g_1(s)$ in terms of $t_1(s)$ we obtain

$$\begin{aligned} [t_1(s)]^{-1} &= \frac{a + b s}{p^2(s)} + \frac{s}{\pi} \int_L \frac{ds'}{s'} \frac{\text{Im } [t_1(s')]^{-1}}{s' - s} \\ &\quad + \frac{s}{\pi} \int_{s_{th}}^{\infty} \frac{ds' - \rho(s')}{s' s' - s} \\ &\simeq \frac{a + b s}{p^2(s)} + \sum_{n=0}^{\infty} C_n \omega^n(s) + R(s, 0), \end{aligned} \quad (23)$$

with the constraint that

$$\sum_{n=0}^{\infty} C_n \omega^n(s=0) = 0. \quad (24)$$

Note that for $m_1 = m_2$, Eq. (23) reduces to Eq. (20) with the proper redefinition of the unknown parameters. The analytical expression for $R(s, 0)$ is given in Eq. (A.4).

2.5. Conformal mapping variables $\omega(s)$

The form of $\omega(s)$ depends on the cut structure of the reaction. Since it is impossible to write a dispersion representation for

the inverse amplitude in the coupled-channel case, we do not include in $\omega(s)$ possible inelastic cuts, as it was proposed in [15, 40]. Therefore $\omega(s)$ is solely specified by the position of the closest left-hand cut branching point (s_L) and an expansion point (s_E), around which the series is expanded, $\omega(s_E) = 0$. The latter typically is chosen in the middle between the threshold and the energy of the last data point that is fitted to the data,

$$\sqrt{s_E} = \frac{1}{2} \left(\sqrt{s_{th}} + \sqrt{s_{max}} \right). \quad (25)$$

This particular choice guarantees a fast convergence of the conformal expansion in that region. To access some of the systematic uncertainties, the value of s_E can be varied around its central value (25).

Since for the scattering of particles with $m_1 = m_2 = m$ the left-hand cut lies on the real axis, $-\infty < s < s_L$, one can use a simple function

$$\begin{aligned} \omega(s) &= \frac{\sqrt{s - s_L} - \sqrt{s_E - s_L}}{\sqrt{s - s_L} + \sqrt{s_E - s_L}}, \\ s_L &= 4m^2 - t_x, \end{aligned} \quad (26)$$

where t_x is the lowest threshold in the crossed t or u channels. For instance for $\pi\pi \rightarrow \pi\pi$ or $D\bar{D} \rightarrow D\bar{D}$ scattering $t_x = 4m_\pi^2$.

For the case when $m_2 > m_1$ (e.g. $\pi K \rightarrow \pi K$ or $\pi D \rightarrow \pi D$ scattering), the left-hand cut structure is a bit more complicated (see Fig. 1). In addition to the left-hand cut lying on the real axis $-\infty < s < (m_2 - m_1)^2$, there is a circular cut at $|s| = m_2^2 - m_1^2$. The conformal map that meets these requirements is defined as

$$\begin{aligned} \omega(s) &= - \frac{(\sqrt{s} - \sqrt{s_E})(\sqrt{s} \sqrt{s_E} + s_L)}{(\sqrt{s} + \sqrt{s_E})(\sqrt{s} \sqrt{s_E} - s_L)}, \\ s_L &= m_2^2 - m_1^2. \end{aligned} \quad (27)$$

We note that for the forms of $\omega(s)$, given in Eqs. (26) and (27), the conformal series, being truncated at any finite order, is bounded asymptotically. This is consistent with the assigned asymptotic behavior.

2.6. Comparison to mIAM

Before applying the dispersive inverse amplitude representations to the physical cases, it is instructive to compare Eqs. (9) and (11) with the mIAM [27]. The latter is a widely used way of unitarizing chiral perturbation theory (ChPT) (see e.g. Refs.[28–30]). For the elastic S-wave scattering it has the following form

$$t_0^{\text{mIAM}}(s) = \frac{[t_0^{\text{LO}}(s)]^2}{t_0^{\text{LO}}(s) - [t_0^{\text{NLO}}(s) - t_0^{\text{LO}}(s)] + A^{\text{mIAM}}(s)} \quad (28)$$

where t_0^{LO} and t_0^{NLO} are leading order (LO) and next-to-leading order (NLO) S-wave scattering amplitudes in ChPT, respectively. Note, that Eq. (28) can be naively derived in the physical region by performing NLO expansion of $\text{Re}[t(s)]^{-1}$ and plugging it into $[t(s)]^{-1} = \text{Re}[t(s)]^{-1} - i\rho(s)$ relation. On

	Fit parameters					$\chi^2/d.o.f$	Pole position	
	g_A	a	b	C_0	C_1		$\sqrt{s_p}$, MeV	$\sqrt{s_p^{\text{Roy-like}}}$, MeV
$\pi\pi \rightarrow \pi\pi$								
$(J = 0, I = 0)$, Exp	0.44	-	-	4.86	-	0.4	$468 - i 239$	$457_{-13}^{+14} - i 279_{-7}^{+11}$
$(J = 0, I = 0)$, Lattice $m_\pi = 236$ MeV	0.55	-	-	1.39	-	0.8	$554 - i 170$	-
$(J = 0, I = 2)$, Exp	-0.84	-	-	-23.98	-	0.0	-	-
$(J = 1, I = 1)$, Exp	-	2.30	-	-5.42	-	3.0	$758 - i 73$	$763.7_{-1.5}^{+1.7} - i 73.2_{-1.1}^{+1.0}$
	-	1.92	-	-4.26	-4.44	0.9	$762 - i 71$	
$(J = 2, I = 0)$, Exp	-	0.04	10.01	-7.87	-	1.1	$1261 - i 94$	$1267.3_{-0.9}^{+0.9} - i 87(9)$
$\pi K \rightarrow \pi K$								
$(J = 0, I = 1/2)$, Exp	0.44	-	-	2.30	-	2.1	$707 - i 246$	$648(7) - i 280(16)$
	0.22	-	-	1.48	1.54	0.0	$684 - i 312$	
$(J = 0, I = 1/2)$, Lattice $m_\pi = 239$ MeV	0.63	-	-	1.53	-	0.4	$764 - i 278$	-
$(J = 0, I = 3/2)$, Exp	-0.86	-	-	-7.86	-	0.5	-	-
$(J = 1, I = 1/2)$, Exp	-	0.86	-1.05	-	-	0.7	$889 - i 27$	$890(2) - i 25.6(1.2)$

Table 1: Fit parameters entering Eqs. (12, 20, 21, 23) which were adjusted to reproduce available pseudo-data from the Roy-like analyses [19, 23] or lattice data [6, 8]. In Eq. (12), the Adler position s_A is fixed from the LO ChPT (given in Eq. (32)), while the subtraction constant is chosen to be at threshold, $\tilde{s}_M = s_{th}$. In the right columns we collect pole positions found on the 2nd Riemann sheet and compare them with the Roy-like extractions [18, 19, 23]. See text for more details.

the other hand, it has been shown in Ref. [27] that Eq. (28) can be justified by writing the p.w. dispersion relation for the inverse amplitude and approximating the subtraction constants and the left-hand cut discontinuity by its chiral expansion. The $A^{\text{mIAM}}(s)$ term is needed to remove a spurious pole below threshold and at the same time incorporate correctly the Adler zero.

By taking LO and NLO SU(2) ChPT amplitudes from [41] with low energy constants from [42] for the isoscalar S-wave $\pi\pi$ scattering we have checked that mIAM given in Eq. (28) indeed satisfies the dispersion relation for the inverse amplitude (11)

$$\begin{aligned}
[t_0^{\text{mIAM}}(s)]^{-1} &= [t_0^{\text{mIAM}}(\tilde{s}_M)]^{-1} + \frac{s - \tilde{s}_M}{s_A - \tilde{s}_M} \frac{g_A}{s - s_A} \\
&+ \frac{s - \tilde{s}_M}{\pi} \int_{L,R} \frac{ds'}{s' - \tilde{s}_M} \frac{\text{Im} [t_0^{\text{mIAM}}(s')]^{-1}}{s' - s}, \\
g_A &= \left(\left. \frac{dt_0^{\text{mIAM}}(s)}{ds} \right|_{s=s_A} \right)^{-1}, \quad (29)
\end{aligned}$$

but not for the direct amplitude (9)¹

$$t_0^{\text{mIAM}}(s) \neq t_0^{\text{mIAM}}(s_M) + \frac{s - s_M}{\pi} \int_{L,R} \frac{ds'}{s' - s_M} \frac{\text{Im} t_0^{\text{mIAM}}(s')}{s' - s}, \quad (30)$$

due to two spurious poles on the 1st Riemann sheet at $s = -0.87 \pm 0.49 i$ GeV². These distance poles break causality and strictly speaking mIAM for the S-wave can not be called a dispersive approach for $t_0(s)$. In contrast, for the P-wave, we

checked that $t_1^{\text{IAM}}(s)$ given by [43]

$$t_1^{\text{IAM}}(s) = \frac{[t_1^{\text{LO}}(s)]^2}{t_1^{\text{LO}}(s) - [t_1^{\text{NLO}}(s) - t_1^{\text{LO}}(s)]}, \quad (31)$$

satisfies both: the p.w. dispersion relations for the inverse amplitude given by Eq. (18) and also the p.w. dispersion relation for the direct amplitude². For $J = 2$, $t_2^{\text{LO}}(s) = 0$ and the IAM requires the knowledge of the next-to-next-to-next-to-leading order chiral amplitude [44], which is not available in the literature. Therefore, we cannot check explicitly whether its representation satisfies (or not) the dispersion representation for the direct amplitude.

The main difference between the proposed dispersive inverse amplitudes given in Eqs. (12, 20, 21, 23) and mIAM (IAM) is that the former can be applied to any elastic scattering, and it is not limited to the Lagrangian based re-summation scheme [45]. The unknown parameters in Eqs. (12, 20, 21, 23) can be fixed directly from the experimental or lattice data (some numerical examples will be shown below). The only required input from ChPT is the Adler zero position, since it lies in the unphysical region and typically can not be constrained well by the data. Furthermore, dispersive inverse amplitudes can be easily applied to describe $J \geq 2$ processes, like e.g. $f_2(1270)$ resonance.

3. Numerical examples

In this section, we present some test fits to the well-established $\pi\pi$ and πK scattering with $J = 0, 1, 2$ in the low

¹The particular choice of $\tilde{s}_M (\neq s_A)$ and s_M is irrelevant. The only constraint is that they should lie inside the region where the amplitude is real.

²The $J = 1$ version of Eq. (9) can be achieved by choosing $s_M = s_{th}$ and setting $t(s_{th}) = 0$ in accordance with Eq. (15).

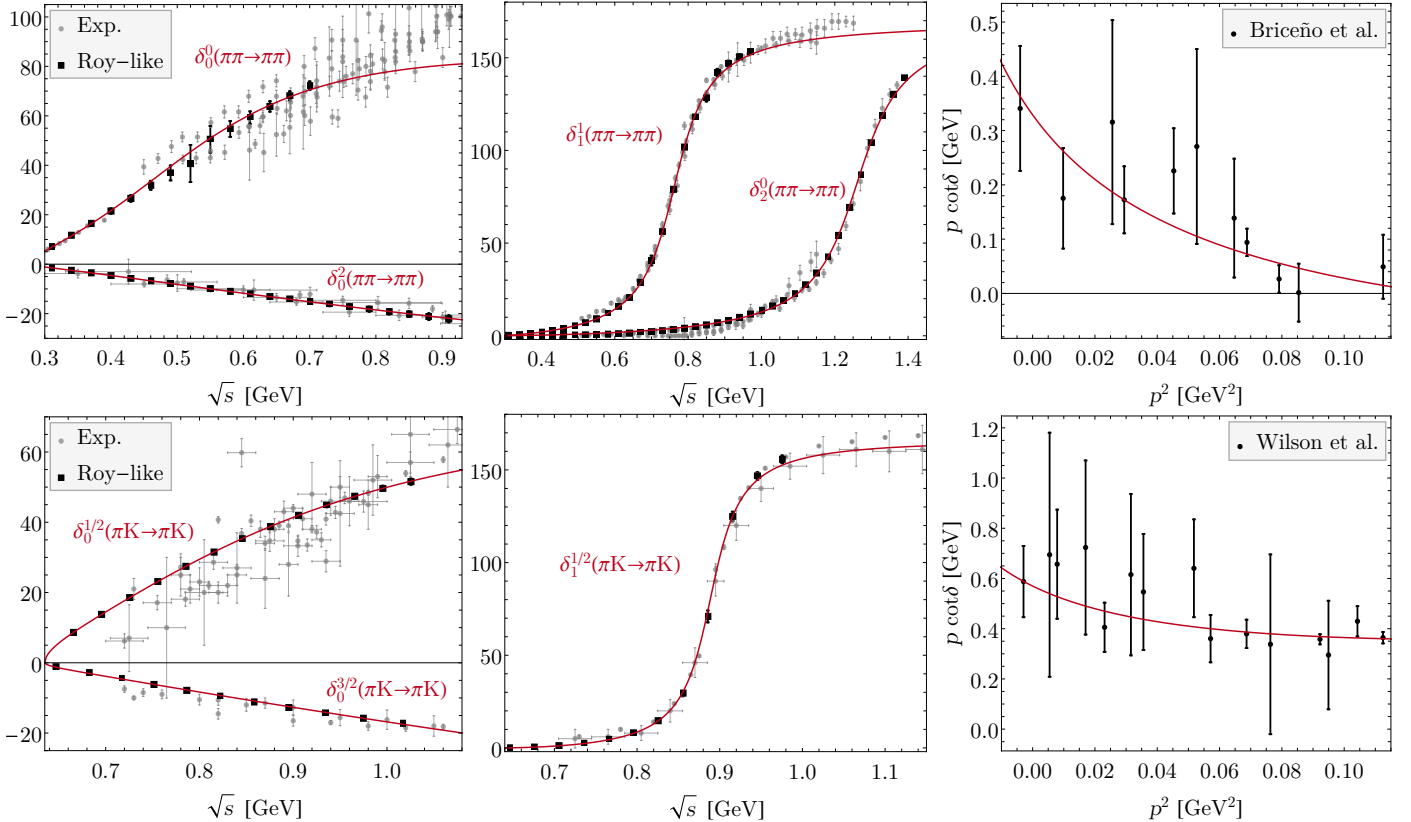


Figure 2: Results of the fits (δ_j^l) to the pseudo-data from the Roy-like analyses (left and central panels) [19, 23] and lattice data (right panels) [6, 8].

energy region. Here we do not attempt to provide a detailed analysis of experimental data. Instead, we opt for fitting the result of the Roy (Roy-Steiner) analyses [19, 23], as the best representation of the data. The goal is to show that the proposed dispersive parametrizations are suitable to the search for poles in the complex plane and can describe both: wide tetraquark states (like $\sigma/f_0(500)$) and relatively narrow quark-antiquark states (like $\rho(770)$ meson).

For the S-wave $\pi\pi$ and πK scattering one has to account for an Adler zero of the amplitude required by chiral symmetry. Its position typically lies very close to the left-hand cut and cannot be determined precisely from the fit to data in the physical region. On the other hand, we have checked that ChPT converges relatively fast around the Adler zero (especially for the physical masses). Therefore for simplicity, we present our numerical test results using the LO input:

$$s_A^{I=0} = \frac{m_\pi^2}{2}, \quad s_A^{I=2} = 2m_\pi^2, \quad s_A^{I=3/2} = m_\pi^2 + m_K^2, \\ s_A^{I=1/2} = \frac{1}{5} \left(m_\pi^2 + m_K^2 + 2\sqrt{4(m_K^2 - m_\pi^2)^2 + m_\pi^2 m_K^2} \right). \quad (32)$$

As one can see in Table 1 and Fig. 2, an accurate description of the Roy (Roy-Steiner) pseudo-data is achieved with at most 3 parameters. We also observed, that adding more terms in the conformal expansion, one can systematically improve the fits. Note that by fitting the Roy (Roy-Steiner) results, which are smooth functions, the $\chi^2/d.o.f$ loses its statistical meaning and can be < 1 .

For the description of the lattice data on S-wave isoscalar $\pi\pi \rightarrow \pi\pi$ ($m_\pi = 236$ MeV) scattering [6] we considered 3 different fits. The first fit is presented in Table 1, where we fixed Adler zero position to LO given in Eq. (32) and provided no error propagation from lattice data. To get an idea of the possible uncertainty, in our second fit, we considered NLO input for s_A with the uncertainty calculated from LECs taken from [42]³. The latter was assumed to be uncorrelated, which leads to a very conservative estimate

$$s_{A,\text{NLO}}^{I=0}(m_\pi = 236 \text{ MeV}) = 0.023(12) \text{ GeV}^2. \quad (33)$$

The propagation of this input into the pole position gives

$$\sqrt{s_p} = 556(5) - i 172(9) \text{ MeV}. \quad (34)$$

In case when both the uncertainties of lattice data and Adler zero input are taken into account (our third fit), one gets

$$\sqrt{s_p} = 553_{-54}^{+47} - i 168_{-15}^{+19} \text{ MeV}, \quad (35)$$

which corresponds to 1σ confidence level provided by the bootstrap analysis. We have also checked that exactly the same result is achieved when only the uncertainty of lattice data is accounted for, while the Adler zero is fixed to its central NLO

³We used SU(2) p.w. amplitudes at NLO from [41] expressed in terms of the pion decay constant in the chiral limit. The one-loop LECs were taken as $l_1^r = -4.03(63) \times 10^{-3}$, $l_2^r = 1.87(21) \times 10^{-3}$, $l_3^r = 0.8(3.8) \times 10^{-3}$ and $l_4^r = 6.2(1.3) \times 10^{-3}$ [42].

position. This points out that the current lattice data completely dominate the uncertainty, and the final result is not very sensitive to the exact position of the Adler zero in Eq.(33).

4. Conclusion and outlook

In this work, we presented novel parametrizations for elastic p.w. amplitudes (see Eqs. (12, 20, 21, 23)), which are based on dispersive representations for the inverse amplitudes. In this approach unitarity and analyticity constraints are implemented exactly. The contributions from the left-hand cuts were accounted for in a model-independent way using the expansion in a conformal variable, which maps the left-hand cut plane onto the unit circle. For the S-wave scattering special attention was paid to the possible Adler zero contribution. For the higher partial waves we implemented carefully the angular momentum barrier factors. We also compared our approach with the mIAM (IAM). We checked numerically that for the S-wave, the mIAM satisfies the dispersive representations for the inverse amplitude, but not for the direct amplitude due to spurious poles on the 1st Riemann sheet.

We applied the novel parametrizations to the well-studied cases of $\pi\pi$ and πK scattering with $J = 0, 1, 2$, showing that at most 3 parameters are needed to reproduce very precise Roy/Roy-Steiner pseudo-data in the physical region. The obtained pole positions lie fairly close to the exact solutions.

The main motivation for developing these amplitudes, which we call dispersive inverse amplitudes (DIA), is their application to the upcoming lattice data in $\pi\pi$, πK , πD and KD channels. In addition, these parametrizations can be beneficial for the fits to data constrained by Roy-like equations or forward dispersion relations [15, 18, 19, 46]. However, the framework is general and not specific to the particular reactions, thus laying the groundwork for analyses of any lattice or experimental data in the elastic region.

The proposed dispersive amplitudes are written in compact analytical forms, which are well-suited for direct numerical implementations. A Mathematica file with these formulas is provided as supplemental material.

Acknowledgements

I.D. acknowledges useful discussions with Cesar Fernández-Ramírez. This work was supported by the Deutsche Forschungsgemeinschaft (DFG, German Research Foundation), in part through the Research Unit [Photon-photon interactions in the Standard Model and beyond, Projektnummer 458854507 - FOR 5327], and in part through the Cluster of Excellence [Precision Physics, Fundamental Interactions, and Structure of Matter] (PRISMA⁺ EXC 2118/1) within the German Excellence Strategy (Project ID 39083149).

Appendix A. Analytic form of $R(s, \tilde{s}_M)$

Here we collect the analytic expressions for

$$R(s, \tilde{s}_M) \equiv \frac{s - \tilde{s}_M}{\pi} \int_{s_{th}}^{\infty} \frac{ds'}{s' - \tilde{s}_M} \frac{-\rho(s')}{s' - s}. \quad (\text{A.1})$$

For $\tilde{s}_M = s_{th}$ it holds [47]

$$R(s, s_{th}) = \frac{\rho(s)}{\pi} \log \left[\frac{\xi(s) + \rho(s)}{\xi(s) - \rho(s)} \right] - \frac{\xi(s)}{\pi} \frac{m_2 - m_1}{m_2 + m_1} \log \frac{m_2}{m_1},$$

$$\xi(s) \equiv 1 - \frac{s_{th}}{s} \quad (\text{A.2})$$

$$\stackrel{m_1=m_2}{=} -\frac{\rho(s)}{\pi} \log \left[\frac{\rho(s) - 1}{\rho(s) + 1} \right],$$

while for any $\tilde{s}_M < s_{th}$ it is given by

$$R(s, \tilde{s}_M) = R(s, s_{th}) - R(\tilde{s}_M, s_{th}). \quad (\text{A.3})$$

Note that for $\tilde{s}_M = 0$, the function $R(s, 0)$ is nothing else, but the well-known one-loop function [38]

$$R(s, 0) = R(s, s_{th}) - R(0, s_{th})$$

$$= R(s, s_{th}) - \frac{1}{\pi} \left(1 + \frac{2m_1 m_2}{m_2^2 - m_1^2} \log \frac{m_2}{m_1} \right) \quad (\text{A.4})$$

$$= -16\pi \bar{J}(s).$$

The numerical implementation of Eq. (A.2) has to be performed with an extra care, since it has to give the correct result not only in the physical region (see Fig. A.3), but also in the complex plane. In the supplemental material we provide the results for $R(s, \tilde{s}_M)$ in Mathematica.

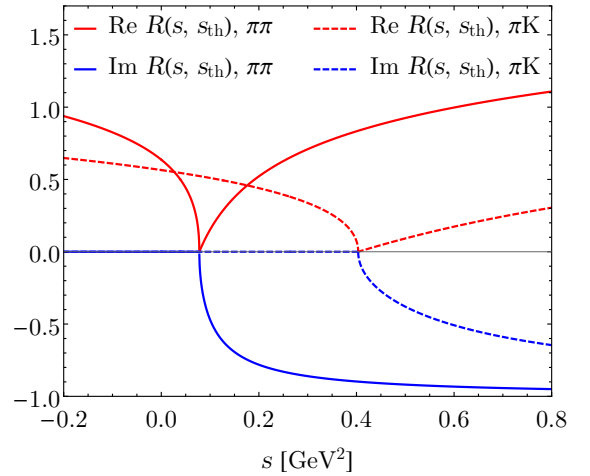


Figure A.3: Real and imaginary parts of $R(s, s_{th})$ for $\pi\pi \rightarrow \pi\pi$ and $\pi K \rightarrow \pi K$ scattering.

References

- [1] R. Aaij et al. (LHCb), Sci. Bull. **65**, 1983 (2020).
- [2] R. Aaij et al., Phys. Rev. Lett. **122**, 222001 (2019); R. Aaij et al., Phys. Rev. Lett. **115**, 072001 (2015).
- [3] C. Adolph et al. (COMPASS), Phys. Lett. B **740**, 303 (2015).
- [4] R. A. Briceno, J. J. Dudek, and R. D. Young, Rev. Mod. Phys. **90**, 025001 (2018); M. R. Shepherd, J. J. Dudek, and R. E. Mitchell, Nature **534**, 487 (2016).
- [5] M. Albaladejo et al. (JPAC) (2021), 2112.13436.
- [6] R. A. Briceno, J. J. Dudek, R. G. Edwards, and D. J. Wilson, Phys. Rev. Lett. **118**, 022002 (2017).

- [7] D. Guo, A. Alexandru, R. Molina, M. Mai, and M. Döring, Phys. Rev. **D98**, 014507 (2018).
- [8] D. J. Wilson, R. A. Briceño, J. J. Dudek, R. G. Edwards, and C. E. Thomas, Physical Review Letters **123** (2019); G. Rendon, L. Leskovec, S. Meinel, J. Negele, S. Paul, M. Petschlies, A. Pochinsky, G. Silvi, and S. Syritsyn, Phys. Rev. D **102**, 114520 (2020).
- [9] L. Gayer, N. Lang, S. M. Ryan, D. Tims, C. E. Thomas, and D. J. Wilson (Hadron Spectrum), JHEP **07**, 123 (2021).
- [10] G. K. C. Cheung, C. E. Thomas, D. J. Wilson, G. Moir, M. Peardon, and S. M. Ryan (Hadron Spectrum), JHEP **02**, 100 (2021).
- [11] S. Prelovsek, S. Collins, D. Mohler, M. Padmanath, and S. Piemonte, JHEP **06**, 035 (2021).
- [12] C. B. Lang, L. Leskovec, D. Mohler, S. Prelovsek, and R. M. Woloshyn, Phys. Rev. D **90**, 034510 (2014).
- [13] D. V. Bugg, Phys. Lett. B **572**, 1 (2003), [Erratum: Phys.Lett.B 595, 556–556 (2004)].
- [14] F. J. Yndurain, R. Garcia-Martin, and J. R. Pelaez, Phys. Rev. D **76**, 074034 (2007).
- [15] J. R. Pelaez and A. Rodas, Phys. Rev. D **93**, 074025 (2016).
- [16] I. Caprini, Phys. Rev. D **77**, 114019 (2008).
- [17] S. Roy, Phys.Lett. **B36**, 353 (1971).
- [18] J. R. Pelaez, Phys. Rept. **658**, 1 (2016).
- [19] R. Garcia-Martin, R. Kaminski, J. Pelaez, J. Ruiz de Elvira, and F. Yndurain, Phys. Rev. D **83**, 074004 (2011); R. Garcia-Martin, R. Kaminski, J. Pelaez, and J. Ruiz de Elvira, Phys.Rev.Lett. **107**, 072001 (2011); J. R. Pelaez, A. Rodas, and J. Ruiz De Elvira, Eur. Phys. J. **C79**, 1008 (2019).
- [20] B. Ananthanarayan, G. Colangelo, J. Gasser, and H. Leutwyler, Phys.Rept. **353**, 207 (2001); I. Caprini, G. Colangelo, and H. Leutwyler, Phys. Rev. Lett. **96**, 132001 (2006); H. Leutwyler, AIP Conf. Proc. **1030**, 46 (2008).
- [21] G. Colangelo, J. Gasser, and H. Leutwyler, Nucl. Phys. **B603**, 125 (2001).
- [22] P. Buettiker, S. Descotes-Genon, and B. Moussallam, Eur.Phys.J. **C33**, 409 (2004); S. Descotes-Genon and B. Moussallam, Eur. Phys. J. **C48**, 553 (2006).
- [23] J. R. Pelaez and A. Rodas, Phys. Rev. Lett. **124**, 172001 (2020); J. Peláez and A. Rodas, Phys. Rept. **969**, 1 (2022).
- [24] I. Danilkin, O. Deineka, and M. Vanderhaeghen, Phys. Rev. D **103**, 114023 (2021); O. Deineka, I. Danilkin, and M. Vanderhaeghen, in *10th International workshop on Chiral Dynamics* (2022), 2203.02215.
- [25] I. Danilkin and M. Vanderhaeghen, Phys. Lett. **B789**, 366 (2019); O. Deineka, I. Danilkin, and M. Vanderhaeghen, Acta Phys. Polon. **B50**, 1901 (2019); I. Danilkin, O. Deineka, and M. Vanderhaeghen, Phys. Rev. **D101**, 054008 (2020); I. Danilkin, M. Hoferichter, and P. Stoffer, Phys. Lett. B **820**, 136502 (2021).
- [26] I. Danilkin, D. A. Molnar, and M. Vanderhaeghen, Phys. Rev. D **102**, 016019 (2020).
- [27] A. Gomez Nicola, J. Pelaez, and G. Rios, Phys. Rev. D **77**, 056006 (2008).
- [28] C. Hanhart, J. R. Pelaez, and G. Rios, Phys. Rev. Lett. **100**, 152001 (2008).
- [29] J. Pelaez and G. Rios, Phys. Rev. D **82**, 114002 (2010).
- [30] J. Nebreda and J. Pelaez., Phys. Rev. D **81**, 054035 (2010).
- [31] S. Mandelstam, Phys.Rev. **112**, 1344 (1958); S. Mandelstam, Phys.Rev. **115**, 1741 (1959).
- [32] G. F. Chew and S. Mandelstam, Phys.Rev. **119**, 467 (1960).
- [33] M. Luming, Phys. Rev. **136**, B1120 (1964).
- [34] P. W. Johnson and R. L. Warnock, J.Math.Phys. **22**, 385 (1981).
- [35] A. Gasparyan and M. F. M. Lutz, Nucl.Phys. **A848**, 126 (2010); I. V. Danilkin, A. M. Gasparyan, and M. F. M. Lutz, Phys.Lett. **B697**, 147 (2011); I. V. Danilkin, L. I. R. Gil, and M. F. M. Lutz, Phys.Lett. **B703**, 504 (2011); A. M. Gasparyan, M. F. M. Lutz, and E. Epelbaum, Eur.Phys.J. **A49**, 115 (2013).
- [36] W. R. Frazer, Phys. Rev. **123**, 2180 (1961).
- [37] A. M. Badalian, L. P. Kok, M. I. Polikarpov, and Y. A. Simonov, Phys. Rept. **82**, 31 (1982).
- [38] A. Gomez Nicola and J. R. Pelaez, Phys. Rev. D **65**, 054009 (2002).
- [39] D. Iagolnitzer, J. Zinn-Justin, and J. B. Zuber, Nucl. Phys. B **60**, 233 (1973).
- [40] J. R. Pelaez and F. J. Yndurain, Phys. Rev. D **71**, 074016 (2005).
- [41] M. Niehus, M. Hoferichter, B. Kubis, and J. Ruiz de Elvira, Phys. Rev. Lett. **126**, 102002 (2021).
- [42] J. Bijnens and G. Ecker, Ann. Rev. Nucl. Part. Sci. **64**, 149 (2014).
- [43] T. N. Truong, Phys. Rev. Lett. **61**, 2526 (1988); A. Dobado, M. J. Herrero, and T. N. Truong, Phys. Lett. **B235**, 134 (1990); T. N. Truong, Phys. Rev. Lett. **67**, 2260 (1991); A. Dobado and J. R. Pelaez, Phys. Rev. D **47**, 4883 (1993).
- [44] A. Dobado and J. R. Pelaez, Phys. Rev. D **65**, 077502 (2002).
- [45] J. R. Peláez, A. Rodas, and J. R. de Elvira, Eur. Phys. J. ST **230**, 1539 (2021).
- [46] J. Pelaez and A. Rodas, Eur. Phys. J. C **78**, 897 (2018).
- [47] D. J. Wilson, J. J. Dudek, R. G. Edwards, and C. E. Thomas, Phys. Rev. D **91**, 054008 (2015).